Transformer Inrush Current Mitigation Techniques for Grid-Forming Inverters Dominated Grids

Abdulrahman Alassi, *Member, IEEE*, Khaled H. Ahmed, Senior Member, *IEEE*, Agusti Egea-Alvarez, Member, *IEEE*, Colin Foote, Member, *IEEE*

***Abstract*— The use of inverters-based resources (IBRs) is rising rapidly in power networks due to increased renewable energy penetration. This requires revisiting of classical network operation standards. For instance, high transformer energization inrush current has been studied extensively under the classical network paradigm. Whereas this paper investigates transformers' energization techniques in the context of inverters dominated grids, where inverters with limited short-circuit current are expected to utilize their grid-forming capabilities for black-start. Common transformer energization techniques such as controlled switching and soft energization are first analyzed with a new perspective aiming to assess their feasibility when used with grid-forming inverters and existing network assets. Parameters influencing soft energization voltage ramp-up time (T_{ramp}) are investigated, and a new T_{ramp} estimation framework for transformer energization from IBRs is introduced. Due to the variability of available point-on-wave circuit breakers (CBs) in distribution networks, controlled energization using single-pole and three-pole CBs is investigated for various configurations and their application limits are identified. A comprehensive case study is then presented using a test network with multiple transformers to benchmark the performance and requirements of each technique when the network is energized from an IBR, followed by a set of practical recommendations.**

***Index Terms*— Black-start, transformers energization, inrush current, controlled switching, soft energization.**

I. INTRODUCTION

CLASSICAL transformers inrush current identification and mitigation techniques have been long presented in the literature, aiming to maintain system reliability and to avoid the mis-operation of protection devices, and continue being studied until today [1, 2]. The rising penetration of inverters-based resources (IBR) to interface renewable energy resources and storage devices into power networks is necessitating a paradigm shift allowing IBRs to provide ancillary services such as black-start. Power inverters are known to have limited overcurrent capability (up to 1.5 pu for short durations) [3]. Identifying suitable inrush current mitigation techniques thus becomes a necessity in the new paradigm rather than a reliability concern. Several inrush current mitigation techniques have been proposed in the literature, ranging in complexity and level of required software/hardware changes. Classical techniques include Pre-insertion Resistors (PIR), which adds to the transformer core flux damping. PIR mainly contributes to: a) reducing the inrush peak, and b) faster transient decay [4]. However, this technique requires additional equipment and increases the overall system cost and footprint. A recent variation aims to utilize virtual damping through grid-forming inverter control (GFC) to mimic the PIR behavior for an offshore windfarm HVDC link [5]. Another recent work proposes modifying the inverter voltage or current references for inrush mitigation. Experimental results using a 1 MVA battery to energize a network show significant inrush mitigation [6]. Though, the presented analysis does not take the residual flux (ϕ_r) impact into account.

Some transformer energization techniques require direct modification to the inverter control to be implemented such as soft energization (SE) through a voltage ramp [7], whereas other techniques require first establishing a 1 pu voltage at the IBR output, followed by inrush mitigation by controlling the circuit breaker (CB) closing instant through controlled switching (CS) [8, 9]. Soft energization from IBRs is recently attracting more industrial and research focus since it exploits the inverters voltage control flexibility. Defining a universally suitable ramping time is a challenging task due to the varying transformer core types, used control, and operating conditions. Several works provide different ramp-rates, ranging from less than a second to tens of seconds [10, 11], with limited justifications. CS technique has also been typically approached in the literature with the assumption that the CB phases can be controlled independently. Although such CBs are available and used with dedicated relays [12], there remains a high number of implemented three-pole (3-PL) CBs, especially in medium and low voltage networks [13]. Since many IBRs are integrated in distribution networks and capable of participating in black-start, industrial efforts are aiming to develop and test solutions

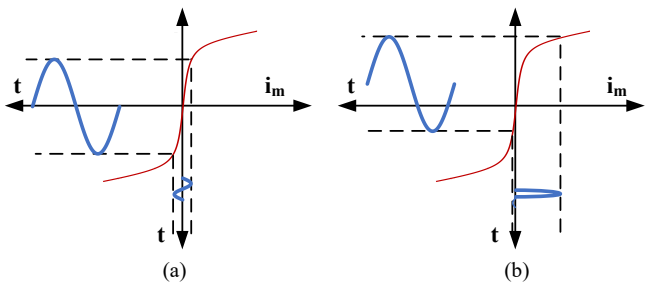

Fig. 1: Visualization of transformer core saturation: (a) normal unsaturated operation, (b) high inrush current in saturated conditions.

Manuscript received May 28, 2022. This work is supported by Iberdrola S.A. as part of its innovation department research activities. Its contents are solely the responsibility of the authors and do not necessarily represent the official views of Iberdrola Group.

Abdulrahman Alassi is with Iberdrola Innovation Middle East, Doha, Qatar (email: aalassi@iberdrola.com). He is also affiliated to University of Strathclyde, Glasgow, UK, along with Khaled Ahmed and Agusti Egea-Alvarez (email: Khaled.ahmed@strath.ac.uk; agusti.egea@strath.ac.uk). Colin Foote was with ScottishPower Energy Networks, Glasgow, UK. He is now with The National HVDC Center, Cumbernauld, UK (email: colin.foote@sse.com).

Color versions of one or more of the figures in this article are available online at http://ieeexplore.ieee.org.

that integrate CS to classical CBs. Such as using dedicated point-on-wave (PoW) relays to control the 3-PL CB closing at instants that could generate minimum inrush across all phases [14]. Implementing CS also requires measuring ϕ_r across all transformer phases. Recent works propose core pre-fluxing before energization to avoid this requirement [15].

The objective of this paper is to present a comprehensive approach that aims to evaluate and identify suitable transformers energization techniques from IBRs under different network conditions and measurements availability. The contributions of this paper are summarized as follows.

- Analysis of CS energization techniques from single-pole (1-PL) and 3-PL CBs, with a focus on the latter type because of its wider availability in distribution networks.
- Proposing a new SE framework that aims to answer the question of how fast a voltage ramp should be set to avoid large inrush currents. The framework is designed to be compatible to large networks with multiple transformers.
- Detailed case study of a practical network, mimicking a distribution network in the United Kingdom, with multiple transformer units. The case study investigates energizing the network from an IBR through CS and SE, showcasing the techniques capabilities and limitations, with recommendations for similar industrial applications based on the presented analysis and findings.

The rest of this paper is organized as follows: section II presents an overview on controlled and soft transformer energization techniques, including 3-PL controlled switching. Then, section III introduces the new T_{ramp} estimation framework for soft energization. Section IV then covers the case study testing methodology and presents the simulation results with detailed analysis. Practical implications of the presented analysis are discussed in Section V, followed by concluding remarks.

II. Transformer Energization Techniques

Energizing a transformer at a random instant can lead to high inrush currents driven by the non-linear transformer saturation characteristics as illustrated in Fig. 1. When the core flux (ϕ) surpasses the linear-region, the magnetizing current increases sharply even against tiny flux increments. Transformer energization techniques aim to avoid conditions leading to the transient core operation in the saturation region. A simplified core flux equation of a single-phase transformer can be derived from the electrical model equivalent illustrated in Fig. 2, with the assumption that secondary winding is open during unloaded energization, and that $X_{LT} \gg R_1$. Such mathematical derivations and simplifications make it easier to infer the flux influencing factors as illustrated in equations (1) and (2).

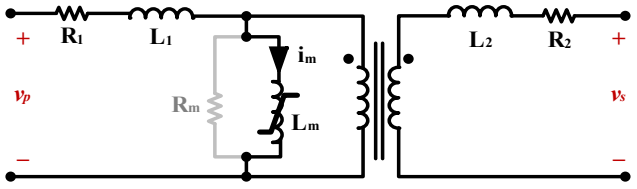

Fig. 2: Single-phase transformer equivalent electrical circuit model.

$$N\frac{d\phi}{dt} + i_m R_1 + L_1\frac{di_m}{dt} = V_P \sin(\omega t + \alpha) \quad (1)$$

$$\phi \approx \frac{-L_m V_P \cos(\omega t+\alpha)}{\sqrt{R_1^2+(\omega L_T)^2}} + \left(\phi_r + \frac{L_m V_P \cos(\alpha)}{\sqrt{R_1^2+(\omega L_T)^2}}\right) e^{-\frac{R_1}{L_T}t} \quad (2)$$

where ϕ is the instantaneous core flux, L_m is the core inductance, and $L_T = L_m + L_1$, N is the transformer turns ratio, ϕ_r is the residual flux in the transformer core, V_P is the energizing side winding voltage amplitude, ω is the angular frequency and α is the energization angle on the voltage waveform. This derivation neglects the parallel shunt R_m branch for simplicity. Equation (2), similar to those reported in [8, 15], presents key flux influencing factors. Though, it should be noted that L_m here is variable between high values in the linear region and very low values during saturation. Approximations such as piecewise expansion of this equation are thus required for detailed time-simulations in a similar fashion to that presented in [17]. The analogy of flux influencing factors in (2) can be extended to three-phase transformers, considering the possible influence between phases and/or the use of single/three core transformers [8, 18].

A. Classical (1-PL-CB) Controlled Switching

This technique, also known classically as Point on Wave (PoW) energization, relies on switching the transformer in the instant when the core residual flux is equal to the 'prospective flux' to eliminate the transient term impact in (2) and neutralize inrush current. The prospective flux (ϕ_{prosp}) is estimated by integrating the voltage at the transformer terminals as in (3). The CB closing scheme requirement under PoW switching is represented in (4). The optimal closing angle (α_{opt}) can be obtained by equating the transient term in (2) to zero and solving for α at t = 0, resulting in (5).

$$\phi_{prosp} = \int V_P \sin(\omega t)\ dt \quad (3)$$

$$CB = 1 \Leftrightarrow (\phi_r = \phi_{prosp}) \quad (4)$$

$$\alpha_{opt} \approx \cos^{-1}(-\phi_{r(pu)}) \quad (5)$$

An illustration for the CS optimal CB closing instant is presented in Fig. 3 for inrush elimination, where ϕ_r is initially set to $-0.7\ pu$. The re-energization signal is sent at $t = 0.06\ s$, and the CB is closed when $\phi_{prosp} = -0.7\ pu\ @\ \alpha \approx 45°$. In this case, the flux moves along the prospective path with no DC component, and the inrush is eliminated. Detailed mathematical derivations for this technique were introduced in [19, 20], and expanded in different research works to include different transformer core types and configurations [21]. When extended to three-phase transformers, the classical CS technique requires independent control of the CB phases to close at their corresponding optimal closing instants. As an example, the existence of a Δ winding at the energizing side requires energizing two CBs first to form a winding voltage, followed by the third CB at the optimal instant that eliminates the inrush current in the remaining two windings.

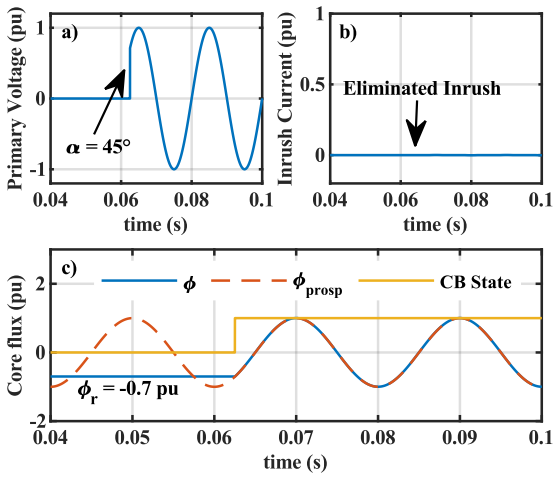

Fig. 3: CS of a single-phase transformer: (a) voltage energizing point, (b) resulting inrush current, (c) ϕ_r and ϕ behavior during energization.

B. Three-pole Breakers Controlled Switching

The independent control of CB phases is not widely implemented in many distribution networks. An industrial example is presented in Distributed ReStart UK project where the use of a 3-PL PoW relay is planned for a large transformer energization in a black-start scenario [22]. The use of such relays implies closing the three CB phases simultaneously, while being able to control a common PoW instant.

Practically, the common PoW closing time should coincide with low prospective flux to residual flux error instants as defined in equation (6) across all phases to achieve good results. The 'good results' terminology here is relative. This is because different transformer cores have different characteristics such as saturation curve knee-point and air-core inductance in their saturation region. That is to say, the same error in (6) can result into two different per unit inrush current magnitudes for two different transformer types. Equation (7) presents a mathematical condition that is derived to approximate the optimal CB closing instant α_{CB} (defined with respect to phase A voltage waveform), based on minimizing simultaneously the errors in each of the three phases. An additional constraint can be added to limit the application to instances where the maximum flux error is ceilinged to avoid excessive inrush. This ceiling is parametrized here as ε_{ceil} to reflect the highlighted variability in transformer core materials.

$$\varepsilon_{\phi} = \phi_r - \phi_{prosp} \tag{6}$$

$$\alpha_{CB} \approx \alpha\left(\min\left(|\varepsilon_{\phi a}| + |\varepsilon_{\phi b}| + |\varepsilon_{\phi c}|\right)\right) : \max\left(\varepsilon_{\phi} < \varepsilon_{ceil}\right) \tag{7}$$

Assuming a low damping factor for the energized transformer, then equation (2) can be used to approximate the worst-case peak flux deviation beyond 1 pu due to the flux error. This is done by setting the time-dependent term in (2) to $\phi_{pk(pu)}$ $(i.e., 1\ pu)$, and substituting the transient term with the per-unit peak flux error from (6) at α_{CB}. Assuming this error is $0.5\ pu$, then the worst-case flux peak occurs around $1.5\ pu$ according to (8).

$$\phi_{pu}(t_{pk}) \approx \phi_{pk(pu)} + \varepsilon_{\phi(pu)} \approx 1 + |\varepsilon_{\phi(pu)}| \tag{8}$$

Practically, the peak flux is less than the value set in (8), to a degree that depends on the circuit damping factor in saturation

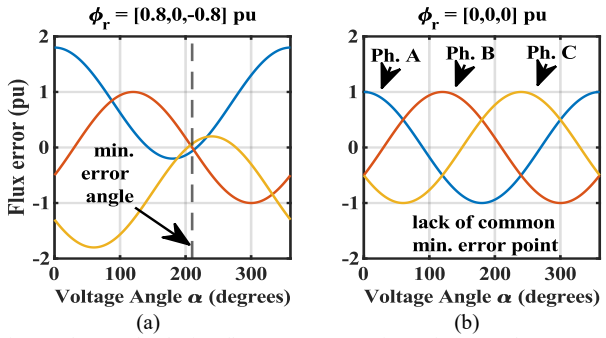

Fig. 4: Three-pole closing flux errors comparison -from (7)- between (a): $\phi_R = [0.8, 0, -0.8]\ pu$, and b) $\phi_R = [0, 0, 0]\ pu$.

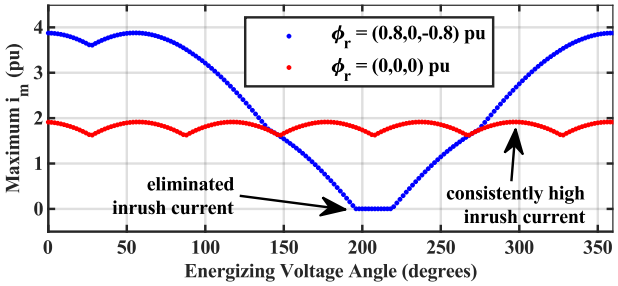

Fig. 5: Three-pole closing peak inrush current at different voltage angles. Each dot on the graph is a distinct power simulation.

region. Though, equation (8) can serve as a first-level approximation to define ε_{ceil} around the flux value resulting in $1\ pu$ inrush current (ϕ_{inr}) in the transformer as in (9).

$$\varepsilon_{ceil(pu)} \approx \left|\phi_{inr_{(pu)}}\right| - 1 \tag{9}$$

Two examples are presented here to illustrate two possible extremes for this technique. In the first example, the residual flux combination is set to $[0.8, 0, -0.8]\ pu$. It is seen in Fig. 4a that a common minimum error point exists for this combination around $\theta_{CB} = 210°$ with $(\varepsilon_{\phi max}\ @\ \alpha_{CB}) \approx 0.065\ pu$ in phase A and C. Closing the three-pole CB at this instant should generate a minimum inrush current in all phases. On the other hand, a different residual flux combination (e.g., zeros in all phases - demagnetized core) is observed to not have a global minimum error points when applying (7) as illustrated in Fig. 4b, and a common angle where the three phases errors ε_{ϕ} have near zero values is missing since $\left(\varepsilon_{\phi max}\ @\ \alpha_{CB}\right) \approx 0.86\ pu$. Many transformers generate high inrush currents when the peak flux is around $1.8\ pu$. Other residual flux combinations between the two reported extremes will exhibit different flux error behaviors, influenced by the existence of common zero (or near-zero) crossing points in all phases.

Simulations are performed to confirm these theoretical predictions, using the standard MATLAB/Simulink transformer model with default saturation characteristics (see Table I) from an ideal voltage source. Here, applying (9) for the transformer model in Table I results in ε_{ceil} estimate around 0.52 pu (above the first case recorded maximum error, and below that from the demagnetized core case). The results of worst-case inrush current scenarios for $0 < \alpha_{CB} < 360°$ are presented in Fig. 5 for both the residual flux combinations presented here, where each dot represents a separate simulation. As expected, the first residual flux sequence $[0.8, 0, -0.8]\ pu$ results into a near-elimination of inrush current around $\alpha_{CB} =$

210°. Whereas the second residual flux sequence $[0, 0, 0]$ results into a pattern of inrush currents that has a global minimum of 1.63 pu, signifying a violation of the transformer rating throughout the complete 360° range for this combination using the standard MATLAB/Simulink model. The same test was performed on three-core and single core transformers in wye and delta configuration with similar results. This consistency is expected since all phases are energized simultaneously. This demonstration serves to illustrate that although 3-PL CS technique can be quite effective in many cases when access to independent phase CBs is not available, it can still lead to significant inrush currents under other residual flux combinations for the whole PoW angles range. This can cause more significant issues when combined with inverters limited overcurrent capabilities.

B. Soft Energization

When applying this technique, the transformer is energized through a ramping voltage between 0 and 1 pu in a period equal to T_{ramp}. Very fast ramps can still cause significant inrush currents, while very slow ramps extend the time during which protection equipment may lack an ability to detect faults due to the voltage being too low. Selecting an appropriate T_{ramp} thus becomes an important task. The applied input voltage across ramping and steady-state stages is defined as in (10).

$$v_p = \begin{cases} \frac{t}{T_{ramp}} V_P \sin(\omega t + \alpha) : t < T_{ramp} \\ V_P \sin(\omega t + \alpha) : t \geq T_{ramp} \end{cases} \quad (10)$$

Numeric simulation tools such as MATLAB or PSCAD can be used to visualize the ramping voltage impact on the flux and inrush current behavior. During the ramp, two opposite actions are observed: flux building-up due to the voltage ramp, and the transient flux exponential decay by the damping factor. To visually demonstrate the behavior during SE, the default MATLAB/Simulink transformer is used with a residual flux combination of $[0.8, 0, -0.8]\, pu$ in a $Y_g - Y_g$ configuration. The transformer is connected to an ideal voltage source to measure the direct soft energization impact. The energization is repeated four times at different ramp-rates with $T_{ramp} = 1\,s, 2\,s, 5\,s\ and\ 10\,s$. The results are summarized in Fig. 6,

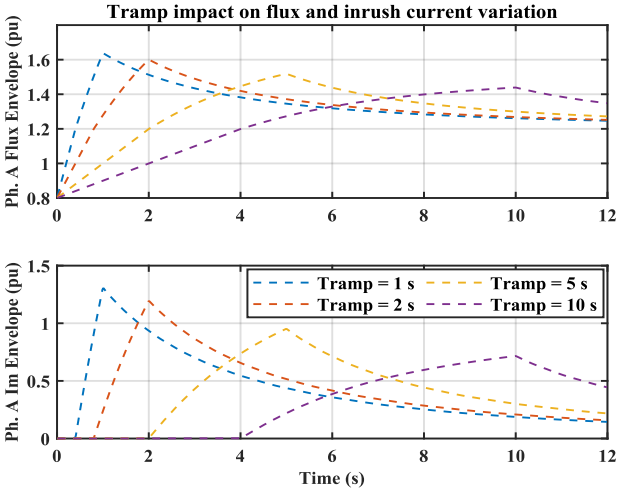

Fig. 6: Impact of varying the voltage ramp time on peak flux and magnetizing current (Ph. A of a Y-Y transformer with $\phi_r = 0.8\, pu$).

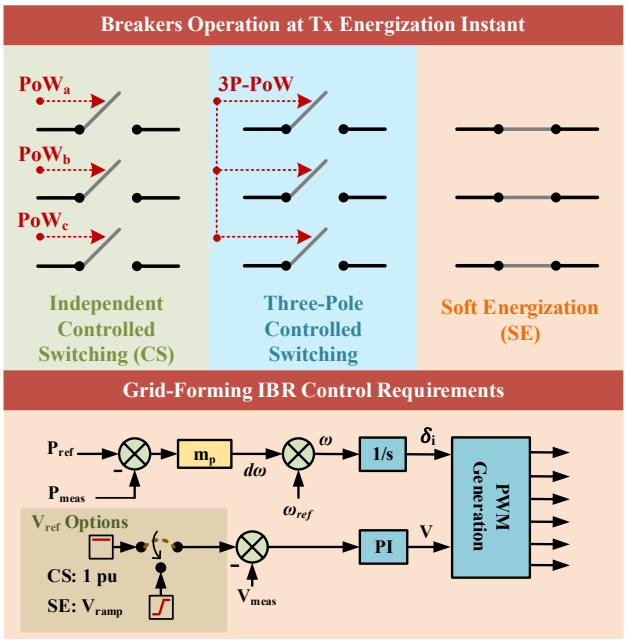

Fig. 7: Breakers and GFC requirements for each energization technique.

which illustrates the absolute peak envelope of both flux and inrush current waveforms for phase A for these different T_{ramp} values. Clearly, the peak flux is reduced as the ramping time increases due to the damping effect of the transient term while the voltage takes longer time to build-up. This results in reduced inrush current magnitude, peaking at $t = T_{ramp}$, before both flux and current continue decaying until the transient term impact is vanished. Although Fig. 6 accurately demonstrates the trends during SE, the results orders-of-magnitude cannot be generalized to all transformer models. However, the key influencing factors can be generalized. These are observed to be: a) residual flux, b) source-to-transformer impedance, c) transformer core characteristics, and d) ramping time.

C. Energization Techniques Benchmark for IBRs

The transformer energization techniques covered in this paper vary significantly in their operation and requirements. For that, a brief high-level comparison for their requirements from GFC and CBs points of view are presented here. The voltage control reference for soft energization should be modified to incorporate and track a ramping reference, whereas CS requires establishing a 1 pu voltage at the transformer CBs input terminals. Fig. 7 summarizes the transformer CBs control arrangements for the different techniques, in addition to the GFC variations using a basic droop loop as a benchmark, based on equations (11)-(13).

$$V_{GFC} = V \angle \delta_i \quad (11)$$

$$V = (V_{ref} - V_{meas})(K_p + \frac{K_i}{s}) \quad (12)$$

$$\delta = \frac{1}{s}\left(\omega_{ref} + m_p\left(P_{ref} - P_{meas}\right)\right) \quad (13)$$

III. New Soft Energization Framework

The framework presented here for T_{ramp} estimation is an extension to that presented in [16]. The new framework is tailored and extended to IBR applications with larger networks

consideration. It aims to answer the questions of how fast a SE ramp should be to limit the peak source current and power to the rated values. Moreover, the framework aims to provide a flexible approach that can impact sizing the inverter if it is yet to be installed mainly for the network energization purposes. The methodology is tailored and extended to grid-forming inverter applications with larger networks consideration that may consist of a single or multiple transformers with various ratings. The proposed framework should mainly be applied before the network energization to provide a suitable ramp-rate recommendation.

The ramping time estimation approach presented here is iterative and model based in nature (i.e., it requires access to the energized transformer and network parameters). Knowledge of the energizing network configuration and the energizing source control is recommended for improved estimation accuracy, such as the impedance between energizing source and transformer terminals (e.g., CBs and cables impedance), transformer saturation characteristics and residual flux, as well as the used source control. This is because flux, being the voltage integral, is influenced by this control. The network model availability requirement is, in principle, not a limiting factor in various cases since many distribution and transmission

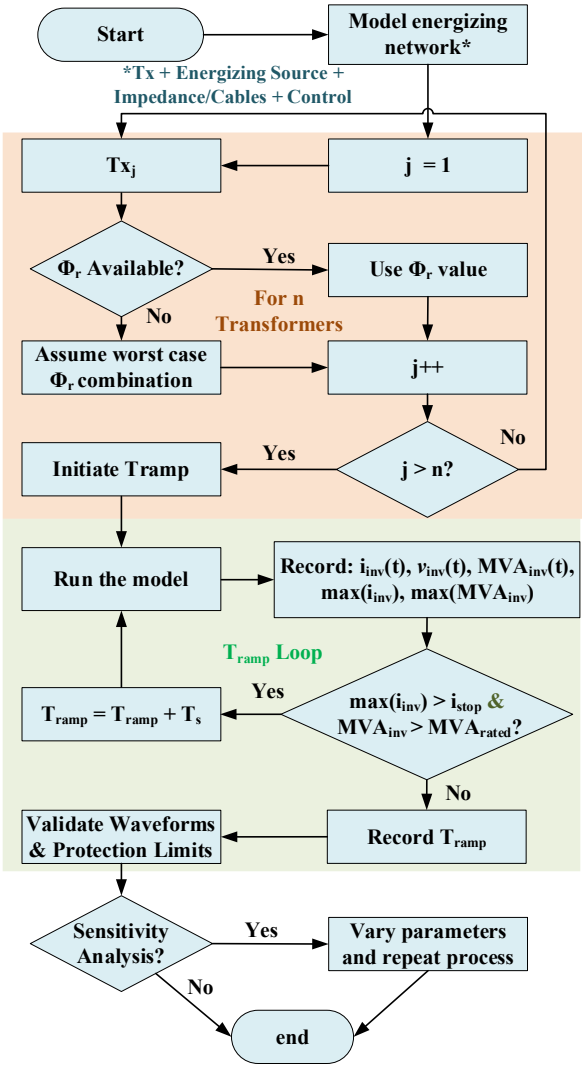

Fig. 8: Flowchart of the proposed T_{ramp} estimation algorithm.

network operators have network models with the key required parameters, this is combined with the emerging network measurements digitalization trend that further increases the available data reliability. That said, in cases where parameters are partially missing (e.g., residual flux measurements), then worst-case assumptions can be used (i.e., to the higher $\phi_{r(pu)}$ end). The framework can be used with various power network simulation tools with automation such as MATLAB/Simulink or PSCAD/EMTDC in combination with Python. The idea here is to iteratively run the simulation while varying T_{ramp} until a stopping criteria is achieved.

The new framework flowchart is presented in Fig. 8, and is configured to accommodate networks with n transformers. To implement the proposed methodology, the network model is first initialized, with all the CBs in the energized routes in their on-state. The worst-case assumptions for missing parameters, if any, are also made at this stage. The soft energization T_{ramp} is set to a minimal value close to zero (e.g., $0.1\ s$) to start the simulation. The peak MVA and source currents (in the three-phases) are recorded and compared to the defined stopping criteria. If this criteria is not satisfied, then T_{ramp} is increased and the process is repeated. Naturally, the next simulation should produce lower peak current and inverter MVA due to the increased ramp-time. The iterations are repeated until the stopping criteria is met, and T_{ramp} is set to the first value meeting this target.

In the new framework, a threshold current i_{stop} is defined to balance between the inverter and the transformers. Equation (14) mathematically defines i_{stop} based on both equipment limits: a) when the inverter rating is the energizing bottleneck (smaller MVA than the smallest energized transformer), and b) when smaller MVA transformers than the inverter rating exists in the network. For instance, if a 10 MVA inverter energizes a string of transformers including a 7.5 MVA unit, then a preferable stopping criteria should consider the transformer rating as well as the inverter to maintain operation within rated boundaries for both the IBR and the transformers, since the small transformer is the energization bottleneck here. This way, the ramping time stopping criteria (i_{stop}) ensures that the inverter and transformer limits are respected. Though, if some transformers are much smaller than the IBR rating (e.g., 10 MVA to 500 kW), then using them to define the stopping criteria could be impractical. In this case, the small units may either be energized separately, or using a ramp-rate that ignores their rating (if their protection can withstand short-term inrush).

$$i_{stop} = \begin{cases} F_s i_{invmax} : MVA_{inv} \leq \min(MVA_{Tx}) \\ F_s i_{Tx_i} : MVA_{inv} > \min(MVA_{T_x}) \end{cases} \quad (14)$$

where MVA_{inv} refers to the source inverter rating, $\min(MVA_{Tx})$ refers to the minimum MVA transformer rating in the network, i_{invmax} is the maximum inverter rated current, i_{Tx_i} is the rated current of the smallest transformer and F_s is a user-defined factor between 0 and 1 that sets the desired stopping-criteria safety 'head-room'. The other stopping criteria is related to the inverter MVA power rating that should also be satisfied. This is because in some cases, the current has been observed to be below its stopping threshold while the peak MVA is slightly higher than the rating due to the non-

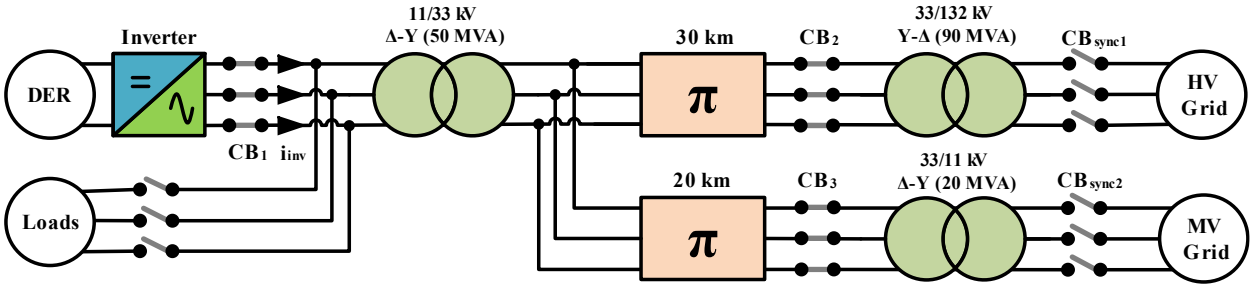

Fig. 9: Block diagram of the network used for the energization case study.

symmetrical nature of inrush conditions and its impact on voltage. The stopping criteria can be defined with respect to flux or transformer magnetizing current if only a single transformer is energized. To maintain generality, the stopping criteria is defined here with respect to the inverter current and rated power due to: a) the limited IBRs overcurrent capability, and b) accommodate the possible existence of multiple transformers in the energized network. A power de-rating factor, similar to F_s, can also be introduced for the inverter MVA rating if high uncertainty is associated with the transformer or network measurements or to comply with network protection requirements in cases where long ramp-durations that are recommended by the framework for a specific MVA rating risk late fault detection outside grid-code limits.

Sensitivity analysis has also been incorporated into the framework and can be optionally coded to run automated testing for different combinations of uncertain parameters, such as different network impedances. This helps in establishing ranges that can be correlated with field results. i_{stop} can also be varied to consider different inverter ratings, taking into account the tradeoff between using small inverters and energizing large transformers, which may lead to higher T_{ramp} when compared to larger (but more costly) inverters.

IV. Network Energization Case Study

A. Test System Description

The methodology to test and benchmark the presented energization techniques in this paper is presented here. First, the network to be energized is illustrated in Fig. 9 . The network is composed of the energizing IBR, transformers with various ratings and configurations, CBs, and cables. The presented transformers combination is used to showcase the energization of multiple transformer topologies. The cables are modeled as $\pi - sections$ with the default MATLAB/Simulink library parameters. The base case network parameters are detailed in Table I. Given the rising penetration of DERs in power networks, assessing the feasibility of using small IBR units in energizing large networks is particularly important for network operators looking for available units for black-start. Hence, a 15 MVA unit is selected for the base case. The current threshold is based on this rating with ($F_s = 0.95$) from Equation 14 for SE investigations. This equates to $0.787\sqrt{2} \times 0.95 = 1.056\ (kA)$ for a 15 MVA inverter at 11 kV.

TABLE I: Test network parameters (for the base case)

Inverter parameters	
Rating (MVA), $f\ (Hz)$	15, 50
$Z_{filter}\ (pu)$	0.075
Z_{filter} X/R ratio	12.5
MATLAB/Simulink Transformer pu parameters	
$R_{p,s}\ (pu)$	0.002
$L_{p,s}\ (pu)$, $L_0\ (pu)$	0.08, 0.5
$R_m\ (pu)$	500
$T_{x1}\ \phi_{r(a,b,c)}\ (pu)$	0.8, 0, -0.8
$T_{x2}\ \phi_{r(a,b,c)}\ (pu)$	-0.4, 0.7, -0.3
$T_{x3}\ \phi_{r(a,b,c)}\ (pu)$	0, 0, 0
Transformers saturation curve	
$i_m\ (pu)$	$[0, 0, 0.0024, 1]$
$\phi\ (pu)$	$[0, 0.85, 1.2, 1.52]$
Cable Parameters (per km)	
$(R, L, C)_{cable}$	12.73 $m\Omega$, 0.93 mH, 12.74 nF

B. Energization Techniques Testing Methodology

Controlled switching in its 1-PL and 3-PL CB forms is tested with the assumption that residual flux and prospective flux measurements are available for all transformers. The delay effect between sending the CB closing command and the actual contact closing instant is ignored and assumed to be properly compensated by the algorithm, a relevant compensation technique example is presented in [23]. The case study assumes that CB_1 is 3-PL CB type, and that CB_2 & CB_3 are 1-PL type CBs. The selected three transformers provide a combination of topologies that cover various scenarios to study their energization under different assumptions. In Fig. 9, the CS sequence in this case study is such that the grid-forming inverter control first provides 1 pu voltage at CB_1 input, then the CB is closed at its combined least flux error point from equation (7). Following the first transformer energization, CB_2 & CB_3 are closed independently to draw least inrush current using separate 1-PL closing algorithms that are adjusted to accommodate their individual configuration. The next black-start step is typically connecting load blocks and synchronizing to the HV and MV grids. A relevant synchronization technique is presented in [24]. In the presented case study, SE is tested under the new defined framework in Section III. CBs between the inverter and the energized transformers are initially closed, and the energization is then simulated while increasing T_{ramp} after each simulation

TABLE II: Network Energization Case Study – Covered Scenarios

Technique	Case #	Parameters Variation from Base Case
Controlled Switching	Case 1	Base Case
	Case 2	$\phi_r(T_{x1}) = [0, 0, 0]$
Soft Energization	Case 1	Base Case
	Case 2	Saturation curve: $i_m = [0, 0, 0.0024, 3]$, $\phi = [0, 0.85, 1.1, 1.52]$
	Case 3	$\phi_r(T_{x1}, T_{x2}, T_{x3}) = [0, 0, 0]$ (Demagnetized cores)

until the stopping criteria is satisfied. The simulations continue here after the stopping criteria is satisfied for improved results visualization and trends identification. The total number of simulations per SE scenario is 34, with $T_{ramp} \in [0.2, 30]\ s$.

C. Test Scenarios Definition

This section presents the network energization case study through multiple scenarios covering CS and SE. The scenarios (and their sensitivity variations) are summarized in Table II. The CS sensitivity case only considers varying the residual flux of the first transformer ($T_{x\,1}$), since it is energized with a 3-PL CB. Varying ϕ_r of the other transformers does not have a noticeable impact since their 1-PL CB are ideally able to track and largely mitigate the inrush impact. Whereas two sensitivity cases are considered for SE: a) varying the core characteristics of all transformers, and b) demagnetizing all transformers by setting ϕ_r to zero across all phases. The first sensitivity case aims to demonstrate the impact of multiple transformer core types with different saturation-curve knee-voltage and air-core inductance, and the second case is considered to demonstrate the paramount impact of residual flux on T_{ramp} selection.

D. Controlled Switching Results

The results for CS testing are presented here, starting with the base network case. T_{x1} is connected to a 3-PL CB with $\phi_r = [0.8, 0, -0.8]\ pu$, while T_{x2} and T_{x3} phases are energized independently. T_{x1} energization is initiated at $t = 0.2\ s$, and the CB is closed at $\alpha_{CB} = 210°$ based on equation (7). Given this ϕ_r combination, the inrush current is nearly zero and the energization occurs smoothly despite the simultaneous phases closing. The two cable segments (30 km and 20 km) are energized simultaneously with T_{x1}. A settling period of 10 cycles is introduced before energizing T_{x2} and T_{x3} to mitigate any transient impact, which may be modified as needed. Then the two remaining transformers are energized. T_{x2} is energized from the Y side, and T_{x3} from the Δ side. The CBs are closed independently at instances when the flux error is around zero, producing near-zero magnetizing currents. A delay of 0.02 s is added between the 1-PL CBs activation for improved visualization. Transformers flux and magnetizing current results at the energization moments for all transformers are summarized in Fig. 10, demonstrating negligible inrush current. The energizing inverter measurements are presented in Fig. 11, showcasing its instantaneous output MVA and current throughout the energization process. The spikes at T_{x1} energization instant are due to the cables energization, since cables can develop their own transient inrush current [25]. In this case study, the cables inrush is within the base inverter rating (below 15 MVA) and peak per-phase current (1.11 kA). If the resulting current exceeds inverter rating, then SE with sufficient T_{ramp} can be used for network energization to mitigate this issue.

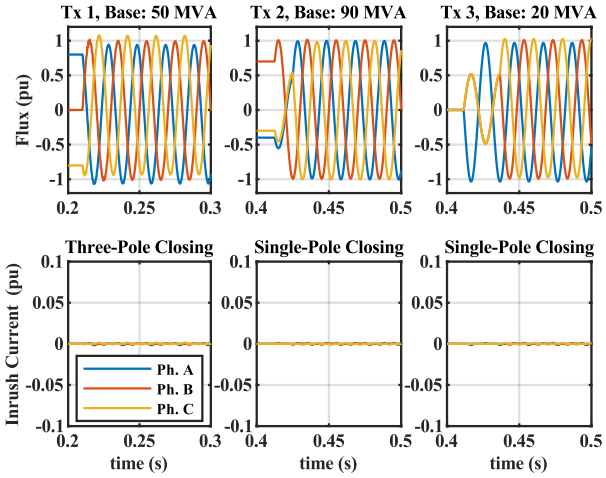

Fig. 10: CS base case: flux & inrush currents at energization points.

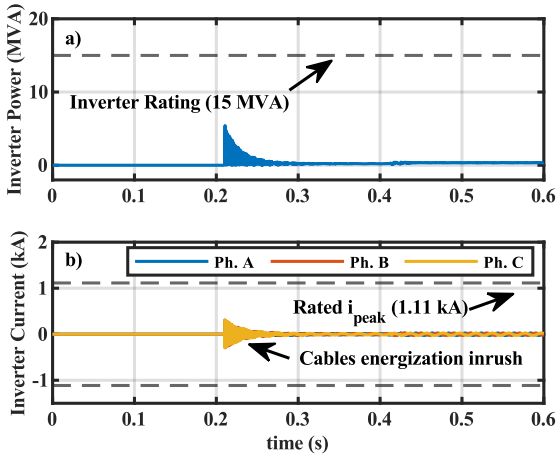

Fig. 11: CS base case: a) IBR peak MVA, b) instantaneous current.

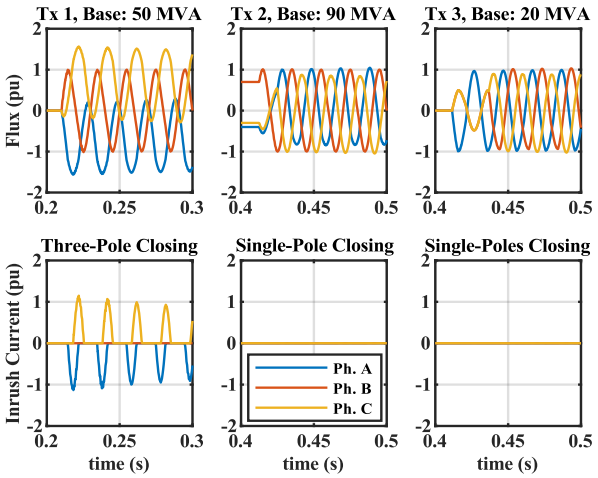

Fig. 12: CS sensitivity case: flux & inrush currents at energization points.

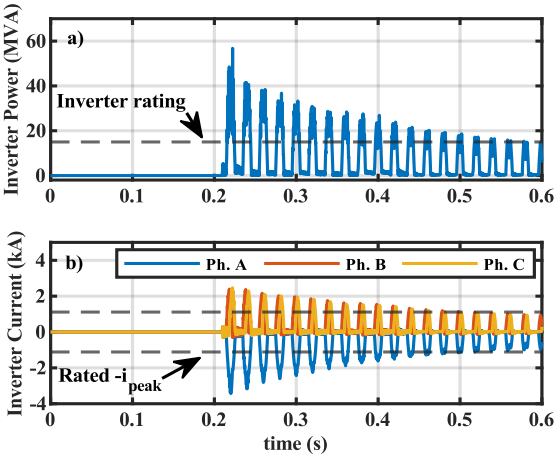

Fig. 13: CS sensitivity case: a) IBR peak MVA, b) instantaneous current.

Controlled Switching Sensitivity Analysis

The sensitivity case presented here tests the network energization performance under a different ϕ_r combination for T_{x1}. The chosen combination [0, 0, 0] generates high minimum common ε_ϕ and inrush current across the full 360° range is illustrated in Fig. 5. T_{x1} is observed here to generate very high inrush current (~ 1 pu) due to the simultaneous phases closing at a high error point for phase A and phase C, as summarized in Fig. 12. The other two transformers exhibit similar behavior to the base case. Overall, the required inrush current from the inverter peaks at 56.8 MVA, severely exceeding the chosen base rating of 15 MVA. The inverter MVA and current output for this scenario are illustrated in Fig. 13. From the presented CS analysis, CB_1 is the network energization bottleneck. Had it been composed of three 1-PL CBs with accurate residual flux measurements, then T_{x1} would have followed a similar behavior as the other two transformers with near-zero inrush current, independent of the ϕ_r combination.

E. Soft Energization Results

SE provides more flexibility in reducing the peak inverter current demand during network energization by selecting an appropriate ramping time. The new T_{ramp} estimation methodology in Fig. 8 is used here. All CBs are initially closed and then the GFC ramping reference is applied. From Fig. 14, the inverter output MVA and current are significantly high for very low T_{ramp} values, as expected. T_{ramp} is increased gradually and the process is repeated while recording the absolute peak inverter MVA and current values. The decreasing trend continues, and the stopping criteria defined by $i_{stop} = 1.056\ kA$ combined with the peak power < 15 MVA is reached around $T_{ramp} = 8\ s$. Fig. 14 also demonstrates the stopping criteria if 10 MVA or 20 MVA inverters are used instead of the adopted 15 MVA inverter. Increasing the rating by 5 MVA can accelerate the ramp to 3 seconds without violating the inverter rating, whereas decreasing the inverter size to 10 MVA requires using a slower ramp of at least 15 seconds to avoid violating the unit rating. This example shows the influence of inverter rating on the ramp-rate selection. The inverter status (existing or to be installed) and the desired use applications may thus be combined with this framework to set an appropriate size under worst-case scenario assumptions for cost optimization.

Looking back at the base 15 MVA inverter rating, time-domain simulation results are presented for $T_{ramp} = 8\ s$. Around this time, the peak inverter power is 14.5 MVA, just below the defined base inverter rating. Time simulation results for this scenario are summarized in Fig. 15, illustrating the ramping and decaying behavior for both apparent power and the inverter current. Since multiple transformers with different ϕ_r are energized, their cores approach saturation region at different times per phase and per transformer. The inverter MVA and current reach their peak at $t = T_{ramp}$, and then continue decaying after the ramp is concluded since the flux transient from this point is primarily influenced by the damping factor.

Soft Energization Sensitivity Analysis

The first sensitivity scenario for SE here considers varying the core saturation curve of the network transformers as in Table II. The sensitivity saturation curve is steeper, with a reduced knee-

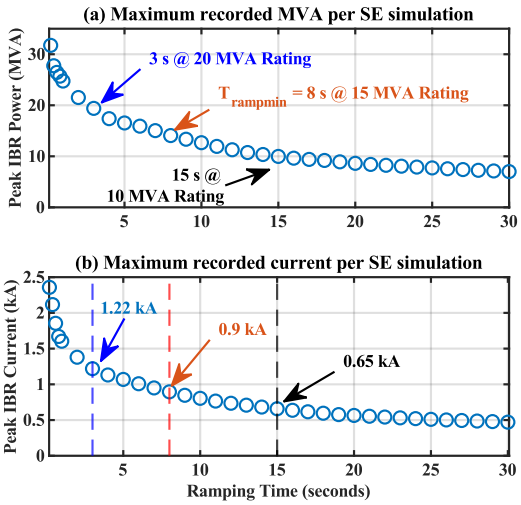

Fig. 14: SE base case: a) peak inverter MVA; b) peak inverter current. Different IBR sizes are also demonstrated for comparison.

voltage from 1.2 pu to 1.1 pu, and increased peak inrush from 1 pu to 3 pu when the flux is 1.52 pu (i.e., decreased air-core inductance). Reducing knee-voltage means that the saturation region is reached faster, while decreasing the air-core inductance leads to higher inrush current per flux increment within the saturation region. The modified ramping time estimation algorithm is re-applied to the network model with the new transformers saturation curve, and the results are summarized in Fig. 16. Longer ramps are required for 10, 15 and 20 MVA inverters in the sensitivity case to avoid violating the IBR ratings. The minimum ramp-time for 20 MVA inverter increased from 3 s in the base case to 8 s here, and from 8 s to 12 s for the 15 MVA inverter. Lastly, the 10 MVA inverter requires a 22 seconds ramp as opposed to the 15 s for the base case. the steeper saturation curve impact is more evident at lower T_{ramp} values. Comparatively, the peak inverter power at $T_{ramp} = 0.2\ s$ is 55.6 MVA compared to 31.7 MVA in the base case (75% increment), whereas at $T_{ramp} = 26\ s$, the difference in peak inverter power diminishes to 18%, between 8.9 MVA for the sensitivity, and 7.5 MVA for the base case. That is, both cases are observed to approach each other as T_{ramp} increases.

The final sensitivity case for soft transformer energization investigates the impact of energizing the studied network when

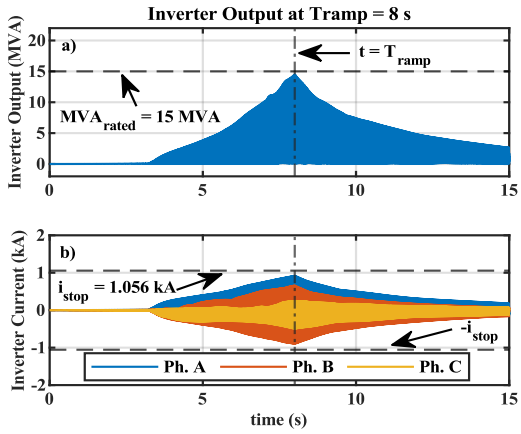

Fig. 15: SE base case instantaneous results with $T_{ramp} = 8\ s$ for: a) IBR power in MVA, b) IBR current for a 15 MVA inverter with $F_s = 0.95$.

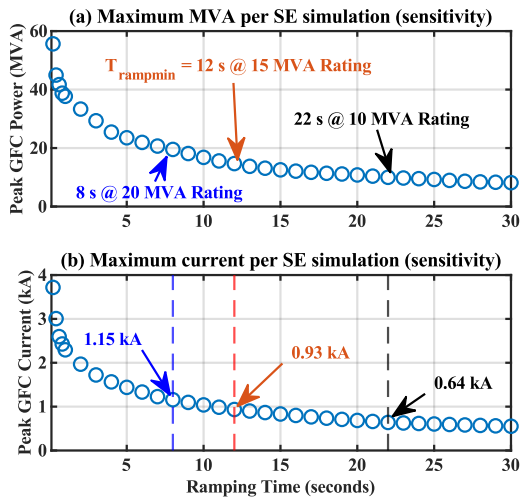

Fig. 16: SE sensitivity case: a) peak inverter MVA; b) peak inverter current. Different IBR sizes are also demonstrated for comparison.

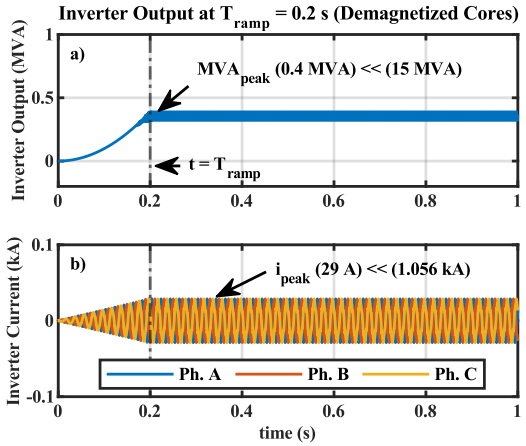

Fig. 17: SE 2nd sensitivity case: instantaneous results for: a) IBR power in MVA, b) IBR current when the network transformers are demagnetized.

all transformers are demagnetized (i.e., with zero residual flux). Since a transformer inrush current is a consequence of the flux reaching saturation region, having demagnetized cores means that the flux must first ramp up from zero to knee-point before causing a noticeable inrush current. This provides a significant headroom that allows for faster ramps, as opposed to the base case where T_{x1} flux in phase A, for instance, is already at 0.8 pu. Meaning that the headroom for the base case is very limited before saturation (between 0.8 pu and 1.2 pu, spanning 0.4 pu), as compared to a 1.2 pu span for the demagnetized core. In this scenario, T_{ramp} is set to 0.2 s only, which is sufficient to suppress energizing inrush current in all three transformers as illustrated in Fig. 17. The peak inverter power in this scenario is around 0.4 MVA, with a peak current of 29 A. The cables in this scenario are also assumed to be initially discharged. This scenario clearly demonstrates the impact of residual flux on SE, and the positive impact of applying the SE technique on demagnetized, or nearly demagnetized (low ϕ_r), transformers.

V. Results Practical Implications

This paper addresses black-start and networks energization provision from IBRs, as part of the rising industrial interest in similar investigations. For instance, the Distributed ReStart industrial project in the UK aims to assess the feasibility of using distributed resources (including IBRs) for black-start. Some distribution areas targeted by this project in the UK are observed to have a concentration of 3-PL CBs with limited PoW relays availability. Thus, the investigation covering CS here aims to answer the question of the 3-PL technique effectiveness against classical CS for similar networks, and to extend the analysis into SE as a potential alternative due to the highlighted IBRs voltage control flexibility. In light of this, key findings and practical/industry implications based on the results reported in this paper are summarized below.

- Classical CS with 1-PL CBs provides superior results to energization from controlled 3-PL CBs. Proper delay compensations for CB closing should be considered for effective CS operation.
- 3-PL CBs can still perform well under a range of ϕ_r combinations (especially at high ϕ_r of $[r, 0, -r]$ form such as [0.8, 0. -0.8] pu), but can still lead to high inrush currents under other combinations (e.g., demagnetized transformers or with low residual fluxes).
- Pre-assessments using (7) and (8) are thus recommended prior to 3-PL CS implementation.
- CS techniques require ϕ_r measurements, which may not be accurately available at all energization points. Industrial relays, such as SynchroTeq [14] may be used (added cost).
- SE can be used as an alternative technique that, in principle, does not require additional installations or measurements.
- SE can also avoid inrush currents resulting from cables energization without requiring additional hardware.
- The presented new framework for T_{ramp} estimation showcases a model-based methodology that can be adopted using industrial software tools such as PSCAD/EMTDC.
- While ϕ_r availability helps achieving better T_{ramp} estimates, it is not a necessity for the new framework implementation since worst-case assumptions for ϕ_r can be made.
- A first worst-case residual flux approximation can be obtained by simultaneously assuming high ϕ_r values across all network transformers. A confirmatory grid-search may also be performed across the transformers, by testing high ϕ_r combinations against a single T_{ramp} value and choosing the aggregate combination with highest inrush current as an input to the ramp-rate estimation framework.
- SE can be used to accommodate the energization process to low IBR ratings through T_{ramp} manipulation (Fig. 14), which provides an economic alternative to the inverters de-rating option, especially when existing IBRs are used.
- That said, high T_{ramp} values should be inspected carefully for the target network and its protection settings/limits to minimize faults non-detection possibility during the ramp when voltage level is below detection thresholds.
- An interesting shown contrast is that soft energization of demagnetized transformers can be smoothly achieved with very fast ramps, whereas high inrush current is obtained when applying 3PL-CS technique with $\phi_r = [0,0,0]\ pu$.

Finally, the results presented in this paper consider a generic single-loop GFC implementation. Preliminary simulations were carried out by the authors in MATLAB/Simulink and RSCAD/RTDS software tools, incorporating inner voltage and

current loops to the inverter control. Results show that for SE, the stopping criteria with inner loops can be achieved with shorter ramp durations due to the imposed current-limiting control dynamics. The results presented recently in [6] support this initial observation, and are recommended for further detailed investigation.

VI. Conclusions

A comprehensive approach has been presented in this paper to assess key transformer energization techniques in IBR dominated power networks, in addition to identifying suitable conditions for their application. The paper also proposed a new framework for soft energization. Given the large number of 3-PL CBs in many IBR-dominated distribution networks, the use of controlled switching through 3-PL CBs is analyzed and shown to be effective over a limited range of residual flux combinations. In contrast, energization from 1-PL CBs can be effective across the full range of residual flux conditions. Though, the application of CS requires accurate ϕ_r measurements and PoW relays, which may not always be readily available. The new framework for estimating the soft energization ramp time, T_{ramp}, considers inverter current protection aspects and the simultaneous energization of multiple transformers. Measurements availability increases the new framework estimation accuracy, but unlike CS, they are not essential for its application. A detailed case study using a network with multiple transformers is presented to benchmark the performance of the different energization techniques. Controlled switching can locally eliminate transformers inrush current, but the inverter can still be prone to inrush currents from long cables if no additional measures such as installing more PoW CBs are considered. With a sufficient T_{ramp} duration, soft energization can prevent the cables energization inrush with no additional required hardware and to mitigate transformers inrush effectively. That said, setting very high ramp-rates may also lead to delays in fault detection until a sufficient source voltage is present.

References

[1] J. E. Holcomb, "Distribution Transformer Magnetizing Inrush Current," *Transactions of the American Institute of Electrical Engineers. Part III: Power Apparatus and Systems,* vol. 80, no. 3, pp. 697-702, 1961.

[2] P. Pachore, Y. Gupta, S. Anand, S. Sarkar, P. Mathur, and P. K. Singh, "Flux Error Function Based Controlled Switching Method for Minimizing Inrush Current in 3-Phase Transformer," *IEEE Transactions on Power Delivery,* 2020.

[3] R. Ierna *et al.*, "Dispatching parameters, strategies and associated algorithm for VSM (virtual synchronous machines) and HGFC (hybrid grid forming convertors)", 19th Wind Integration workshop, Dublin, 2019.

[4] A. Jain, O. Saborío-Romano, J. Sakamuri, and N. Cutululis, "Blackstart from HVDC-connected offshore wind: Hard versus soft energization," *IET Renewable Power Generation,* vol. 15, no. 1, pp. 127-138, 2021.

[5] A. Jain, O. Saborio-Romano, J. Sakamuri, and N. Cutululis, "Virtual Resistance Control for Sequential Green-start of Offshore Wind Power Plants," *IEEE Transactions on Sustainable Energy,* 2022.

[6] M. Shahparasti, H. Laaksonen, K. Kauhaniemi, P. Lauttamus, S. Strandberg, and J. Strandberg, "Inrush Current Management During Medium Voltage Microgrid Black Start with Battery Energy Storage System," *IEEE Access*, 2022.

[7] E. Bikdeli, M. R. Islam, M. M. Rahman, and K. M. Muttaqi, "State of the Art of the Techniques for Grid Forming Inverters to Solve the Challenges of Renewable Rich Power Grids," *Energies,* vol. 15, no. 5, 2022.

[8] J. Mitra, X. Xu, and M. Benidris, "Reduction of Three-Phase Transformer Inrush Currents Using Controlled Switching," *IEEE Transactions on Industry Applications,* vol. 56, no. 1, pp. 890-897, 2020.

[9] H. Ni, S. Fang, and H. Lin, "A Simplified Phase-Controlled Switching Strategy for Inrush Current Reduction," *IEEE Transactions on Power Delivery,* vol. 36, no. 1, pp. 215-222, 2021.

[10] A. Roscoe *et al.*, "Practical Experience of Providing Enhanced Grid Forming Services from an Onshore Wind Park", 18th Wind Integration Workshop, DUblin, 2019.

[11] J. Glassmire, S. Cherevatskiy, G. Antonova, and A. Fretwell, "Using Virtual Synchronous Generators to Resolve Microgrid Protection Challenges," in *2021 74th Conference for Protective Relay Engineers (CPRE)*, 22-25 March 2021 2021, pp. 1-7.

[12] "Switchsync PWC600 Point-on-Wave Controller - Product Report," Hitachi Energy, 2021.

[13] R. Cano-González, A. Bachiller-Soler, J. Rosendo-Macías, G. Álvarez-Cordero, "Optimal gang-operated switching for transformer inrush current reduction," *Electr. Power Syst. Res.,* vol. 131, pp. 80-86, 2016.

[14] T. Rastall, "SynchroTeq - 3-Pole Transformer Switching," Enspec, United Kingdom, 2020.

[15] Y. Pan, X. Yin, Z. Zhang, B. Liu, M. Wang, and X. Yin, "Three-Phase Transformer Inrush Current Reduction Strategy Based on Prefluxing and Controlled Switching," *IEEE Access,* vol. 9, pp. 38961-38978, 2021.

[16] A. Alassi, K. Ahmed, A. Egea-Alvarez, and C. Foote, "Soft Transformer Energization: Ramping Time Estimation Method for Inrush Current Mitigation," in *2021 UPEC Conference*, 31 Aug.-3 Sept. 2021, pp. 1-6.

[17] S. Jazebi, F. d. León, and N. Wu, "Enhanced Analytical Method for the Calculation of the Maximum Inrush Currents of Single-Phase Power Transformers," *IEEE Transactions on Power Delivery,* vol. 30, no. 6, pp. 2590-2599, 2015.

[18] D. Bejmert, M. Kereit, and K. Boehme, "Controlled energization procedures of power transformers," *International Journal of Electrical Power & Energy Systems,* vol. 135, p. 107555, 2022.

[19] J. H. Brunke and K. J. Frohlich, "Elimination of transformer inrush currents by controlled switching. I. Theoretical considerations," *IEEE Transactions on Power Delivery,* vol. 16, no. 2, pp. 276-280, 2001.

[20] J. H. Brunke and K. J. Frohlich, "Elimination of transformer inrush currents by controlled switching. II. Application and performance considerations," *IEEE Transactions on Power Delivery,* vol. 16, no. 2, pp. 281-285, 2001.

[21] U. Parikh and B. R. Bhalja, "Mitigation of magnetic inrush current during controlled energization of coupled un-loaded power transformers in presence of residual flux without load side voltage measurements," *International Journal of Electrical Power & Energy Systems,* vol. 76, pp. 156-164, 2016.

[22] "Distributed ReStart: Power Engineering and Trials - Demonstration of Black Start from DERs Part 1," National Grid ESO, UK, 2021.

[23] G. Benmouyal, N. Fischer, D. Taylor, M. Talbott-Williams, and R. Chowdhury, "A Unified Approach to Controlled Switching of Power Equipment," in *72nd Annual Georgia Tech Protective Relaying Conference*, USA, 2018.

[24] A. Alassi, K. Ahmed, A. Egea-Alvarez, and C. Foote, "Modified Grid-forming Converter Control for Black-Start and Grid-Synchronization Applications," in *2021 UPEC Conference*, 31 Aug.-3 Sept. 2021, pp. 1-5.

[25] I. Lafaia, M. T. C. de Barros, J. Mahseredjian, A. Ametani, I. Kocar, and Y. Fillion, "Surge and energization tests and modeling on a 225kV HVAC cable," *Electric Power Systems Research,* vol. 160, pp. 273-281, 2018.

Abdulrahman Alassi (Member, IEEE) received his B.Sc. and M.Sc. in Electrical Engineering from Qatar University in 2014 and 2016, respectively. He is currently working towards his Ph.D. degree in Electronic and Electrical Engineering from the University of Strathclyde. He previously worked as a researcher at Qatar University between 2014 and 2017. He then joined Iberdrola's innovation center in Qatar where he currently leads the energy systems group. He has published more than 20 articles in technical journals and international conferences and received the best paper award in the 2019 IEEE SGRE Conference. His research interests include converters control, power system studies, Power Hardware-in-the-Loop (PHiL) validation, and the techno-economic optimization of renewables and storage integration.

Khaled H. Ahmed (M'09-SM'12) received the B.Sc. (Hons.) and M.Sc. degrees from Alexandria University, Egypt, in 2002 and 2004, respectively, and the Ph.D. degree in power electronics applications from the University of Strathclyde, U.K., in 2008. He was appointed as a Professor at Alexandria University, in 2019. He is currently a Reader in power electronics with the University of Strathclyde. He has published more than 160 technical articles in refereed journals and conferences as well as a published textbook titled High Voltage Direct Current Transmission: Converters, Systems and DC Grids, a book chapter contribution, and holds a PCT patent PCT/GB2017/051364. His research interests include renewable energy integration, high power converters, offshore wind energy, dc/dc converters, HVDC, and smart grids. He is a Senior Member of the IEEE Power Electronics Society and the IEEE Industrial Electronics Society.

Agusti Egea-Alvarez (Member, IEEE) received the B.Sc., M.Sc., and Ph.D. degrees from the Technical University of Catalonia, Barcelona, in 2008, 2010, and 2014, respectively. In 2015, he was Marie Curie Fellow with China Electric Power Research Institute (CEPRI). In 2016, he joined Siemens Gamesa as a Converter Control Engineer, working on grid forming controllers and alternative HVDC schemes for offshore wind farms. He has been a member of the Power Electronics, Drives and Energy Conversion (PEDEC) Group, since 2018. He is currently a Senior Lecturer with the Department of Electronic and Electrical Engineering at the University of Strathclyde. His current research interests include the control and operation of high-voltage direct current systems, renewable generation systems, electrical machines, and power converter control.

Colin Foote (Member, IEEE) received MEng and PhD degrees in electrical engineering from the University of Strathclyde, UK, in 1999 and 2006 respectively. He is currently a Senior Simulation Engineer at the National HVDC Centre, UK. Previous roles include System Analysis manager at network operator SP Energy Networks and Head of Power Systems at solutions provider Smarter Grid Solutions. He also worked at Mott MacDonald as a power systems analyst and at the University of Strathclyde as a research fellow. He has extensive and varied experience in consultancy, research, management, project design and delivery, solutions development, and training. Research interests focus on power system modeling, simulation and analysis, transmission and distribution network planning, HVDC, distributed generation, and wind power.